Arabidopsis peroxidase AtPRX53 influences cell elongation and susceptibility to *Heterodera schachtii*

Jing Jin,[1,2] Tarek Hewezi[1] and Thomas J. Baum[1,2,*]

[1]Department of Plant Pathology and Microbiology; [2]Molecular, Cellular and Developmental Biology Graduate Program; Iowa State University; Ames, IA USA

Cyst nematodes establish and maintain feeding sites (syncytia) in the roots of host plants by altering expression of host genes. Among these genes are members of the large gene family of class III peroxidases, which have reported functions in a variety of biological processes. In this study, we used Arabidopsis-*Heterodera schachtii* as a model system to functionally characterize peroxidase 53 (*AtPRX53*). Promoter assays showed that under non-infected conditions *AtPRX53* is expressed mainly in the root, the hypocotyl and the base of the pistil. Under infected conditions, the *AtPRX53* promoter showed upregulation at the nematode penetration sites and in their migration paths. Interestingly, strong GUS activity was observed in *H. schachtii*-induced syncytia during the early stage of infection and remained strong in the syncytia of third-stage juveniles. Also, *AtPRX53* showed upregulation in response to wounding and jasmonic acid treatments. Manipulation of *AtPRX53* expression through overexpression and knockout mutation affected both plant morphology and nematode susceptibility. While *AtPRX53* overexpression lines exhibited short hypocotyls, aberrant flower development and reduced nematode susceptibility to *H. schachtii*, the *atprx53* mutant showed long hypocotyls and a 3-carpel silique phenotype as well as a non-significant increase of nematode susceptibility. Taken together these data therefore indicate diverse roles of AtPRX53 in the wound response, flower development and syncytium formation.

Introduction

Cyst nematodes are sedentary obligate biotrophic plant parasites that cause severe yield loss to crops worldwide.[1] Infective second-stage juveniles (J2) penetrate roots and then migrate intracellularly in search of a suitable location to initiate a feeding site, called a syncytium. The formation of the syncytium is a tightly controlled process involving both the parasite and the host plant. While nematode effector proteins, which are produced in the esophageal gland cells and secreted into host plant cells through the nematode stylet, are critical for the establishment of the feeding sites and nematode parasitism,[2-6] host factors also are pivotal in this process.[7] Genome-wide expression profiling of the plant response to cyst nematodes resulted in the identification of genes that are regulated by cyst nematode infection.[8-12] Despite considerable progress in the identification of host genes responsive to cyst nematode infection, little is known about the functional roles of most of these genes during parasitism. Examination of plant genes differentially expressed in response to cyst nematode infection revealed that members of the peroxidase gene family frequently are among the highly responsive genes,[8,12] which suggested important roles during parasitism.

The peroxidase superfamily is divided into three distantly related structural classes.[13] class I encompasses intracellular proteins and can be found in most living organisms but not in animals. These peroxidases function mainly in detoxifying excess H_2O_2.[14] Class II peroxidases are found exclusively in fungi and mostly act in degrading soil debris.[15] Class III peroxidases are found in land plants and contain N-terminal signal peptides for secretion to the cell wall or vacuoles.[16-18] Genes coding for class III peroxidases have been duplicated extensively during evolution and thus form large gene families in all land plant species studied.[16] Some of these enzymes have been shown to be involved in a wide range of physiological and developmental processes, which include cross-linking of cell wall components during cell wall formation and modification,[19,20] lignification,[21,22] suberization[23] and auxin catabolism.[24] Accumulated experimental evidence also implicates class III peroxidases in plant defense responses to pathogen/pest attacks, such as bacteria,[25-27] fungi,[28] viruses,[29] insects[30] and cyst nematodes.[31] Two major functional roles have been attributed to class III peroxidases in response to pathogen attack. The first role is the cross-linking of cell wall components, which strengthens cell walls to impede pathogen invasion.[32,33] A second role lies in the ability to generate reactive oxygen species (ROS) that produce adverse circumstances for pathogen survival[26,34] and/or trigger downstream signaling pathways to activate additional defense mechanisms.[35,36]
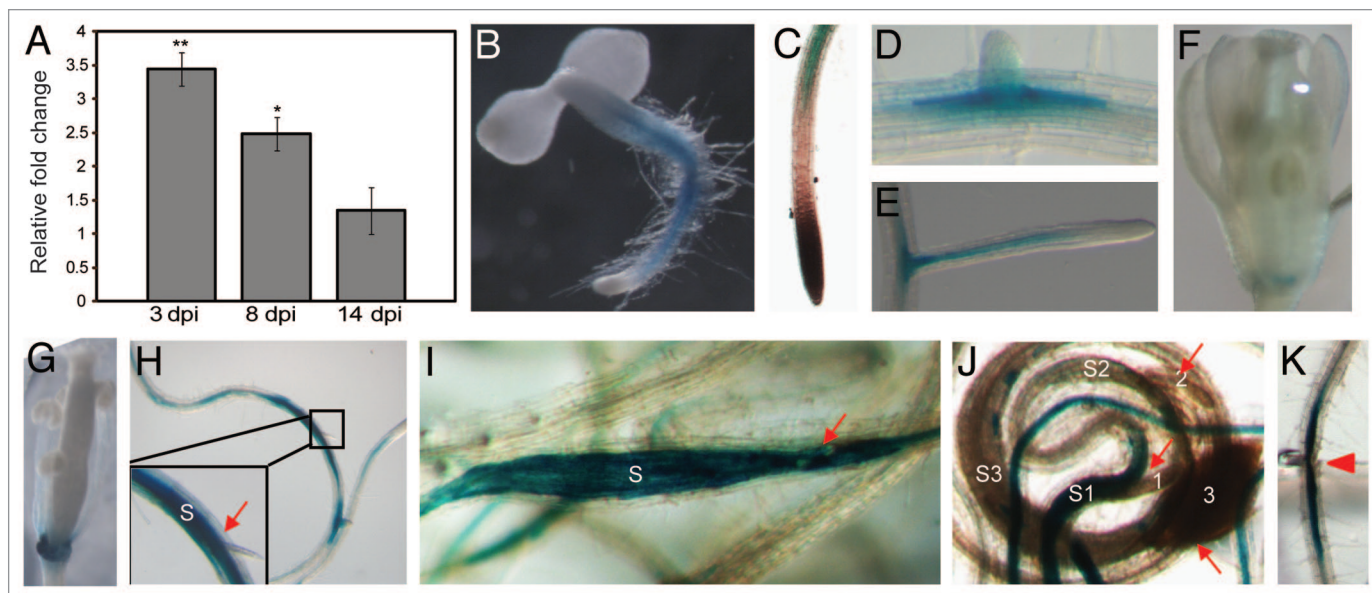
Figure 1. Expression analysis of *AtPRX53* in response to nematode infection. (A) Upregulation of *AtPRX53* mRNA in wild-type Arabidopsis (Col-0) roots in response to *Heterodera schachtii* infection relative to the non-infected control. The expression levels of *AtPRX53* were quantified by quantitative real-time RT-PCR (qPCR) in root tissues of wild-type plants. Infected and non-infected roots were collected at 3, 8 and 14 d post inoculation (dpi). Data are averages of three biologically independent experiments. *Actin8* was used as internal control to normalize mRNA expression levels. Mean values significantly different from the non-infected control were determined by unadjusted paired t-tests. Asterisks indicate mean fold-changes significantly different from those of non-infected wild-type roots (p < 0.05). (B–K) Histochemical localization of GUS activity in transgenic Arabidopsis plants harboring the p*AtPRX53:GUS* construct. Three independent homozygous T$_3$ lines expressing the p*AtPRX53:GUS* construct were generated, and GUS activity was histochemically analyzed in both non-infected and infected plants. (B) through (G), GUS staining in non-infected plants. Whole mount (B), close-up of main root tip (C), emerging lateral root (D and E), flower (F) and developing silique (G). (H) through (J), GUS staining in plants infected with *Heterodera schachtii*. Arrows point to nematodes and S indicates syncytium. Three days post inoculation (dpi) (H), 8 dpi (I) and 14 dpi (J), J3 nematode (1) with syncytium (S1); male (2) with syncytium (S2); mature female (3) with syncytium (S3). (K) GUS staining in root tissue wounded by stabbing with a needle. Arrowhead points to the site of wounding.

The Arabidopsis (*Arabidopsis thaliana*) genome contains 73 genes predicted to encode class III peroxidases, of which only few have been functionally characterized.[17,35,37] A further understanding of peroxidase functions, thus, is of prime interest. One member of the Arabidopsis class III peroxidase gene family, *AtPRX53*, previouly has been shown to be upregulated by *Heterodera schachtii* infection.[8,12] In the current study, we addressed the potential role of *AtPRX53* during plant-nematode interactions. Using promoter activity assays we showed that *AtPRX53* is strongly upregulated in *H. schachtii*-induced feeding sites during early infection. Gain- and loss-of-function mutations showed effects on plant morphology as well as on susceptibility to *H. schachtii*. Analysis of all data presented here suggests that *AtPRX53* most likely is involved in cross-linking of cell wall compounds during *H. schachtii*-induced syncytium growth.

Results

AtPRX53 is upregulated in response to *Heterodera schachtii* infection, wounding and jasmonic acid treatment. To begin investigating the function of *AtPRX53* in the plant response to cyst nematode infection, we used quantitative real-time RT-PCR (qPCR) assays to assess the mRNA expression profile using gene-specific primers designed to discriminate between different members of the peroxidase gene family. Ten-day-old wild-type Arabidopsis seedlings (Col-0) were inoculated with *H. schachtii*, and root tissues were harvested from both infected and non-infected plants at 3, 8 and 14 d post inoculation (dpi) for RNA extraction. Data from three independent experiments showed significant upregulation of *AtPRX53* in *H. schachtii*-infected roots at 3 and 8 dpi relative to non-infected roots (**Fig. 1A**), thus, confirming the 3 dpi observation of Puthoff et al. At 14 dpi, *AtPRX53* mRNA abundance was decreased to non-infected control levels (**Fig. 1A**).

In order to identify where the *AtPRX53* gene was expressed in the developing plant and infected roots, we generated transgenic Arabidopsis lines expressing the β-glucuronidase (GUS) reporter gene under the control of the *AtPRX53* promoter. Three independent transgenic lines were analyzed and showed similar results. Under non-infected conditions, GUS activity was detected in the vascular tissues of the primary root but not in the meristem or the elongation zone of 3-d-old plants (**Fig. 1B and C**). GUS staining was also observed in the lateral roots 10-d-old plants (**Fig. 1D and E**). In shoots of non-infected plants, GUS activity was discovered in the hypocotyl (**Fig. 1B**), the base of the pistil (**Fig. 1F**), and the internode of the silique (**Fig. 1G**). Under infected conditions, the *AtPRX53* promoter showed activity at the site of root penetration of nematodes and in their migration paths (data not shown). Strong GUS activity was detectable in *H. schachtii*-induced syncytia as early as 3 dpi

(**Fig. 1H**), which was sustained also at 8 dpi (**Fig. 1I**). At 14 dpi, GUS activity remained strong in the syncytia of third-stage juveniles, but only weak or no GUS staining could be detected in the syncytia of fourth-stage females or males (**Fig. 1J**). These data implicated *AtPRX53* in playing a role in the wound response and syncytium initiation and development.

Because we observed GUS activity at the sites of nematode penetration and migration, we tested whether the expression of *AtPRX53* can also be activated in response to wounding alone. Roots of p*AtPRX53:GUS* seedlings were wounded, and 3 d post treatment GUS activity was histochemically assayed. GUS expression increased around wounding sites (**Fig. 1K**), which suggested that activation of *AtPRX53* is part of the plant wound response associated with the early infection process.

Since jasmonic acid (JA) is well known as an essential signal in wound-induced gene expression, we assessed whether the *AtPRX53* promoter contains JA-responsive cis-elements by scanning the *AtPRX53* promoter region using the PLACE (Plant cis-acting elements) database.[38] Two JA-responsive cis elements[39] were identified (**Table 1**), potentially explaining the wound-responsiveness of the *AtPRX53* promoter. We further investigated the mRNA expression level of *AtPRX53* in response to JA treatment. In this experiment, 10-d-old Arabidopsis wild-type seedlings were treated with 100 μM methyl jasmonic acid (MeJA), and after 48 h, root tissues were collected for RNA extraction and qPCR analyses. Data obtained from three biological samples revealed a statistically significant 35-fold upregulation of *AtPRX53* in MeJA-treated roots compared with the non-treated control. Also, our analysis revealed that the *AtPRX53* promoter contains other stress-responsive elements including ethylene-[40,41] and ABA-[42] responsive cis-elements as well as two nematode boxes described by Escobar et al. (**Table 1**). Though these regulatory cis-elements are potentially interesting, their functionality was not pursued further in this study.

Morphology and nematode susceptibility as a function of altered *AtPRX53* expression. To study the phenotypic effects of altered *AtPRX53* expression, we obtained a Ds transposon
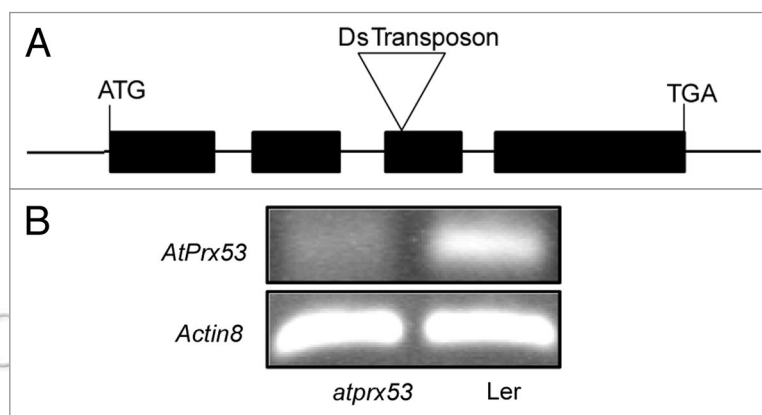

Figure 2. Characterization of the Arabidopsis *atprx53* mutant. (A) Schematic representation of the *atprx53* mutant allele used in this study showing the location of Ds transposon insertion. Black boxes indicate exons and lines between black boxes indicate introns. *AtPRX53* encompasses four exons and three introns and the Ds transposon is located at the third exon, 550 bp downstream of the translation start codon. The translation start codon (ATG) and stop codon (TGA) are indicated. (B) *AtPRX53* mRNA accumulation in the *atprx53* mutant. *AtPRX53* mRNA abundance was determined by qPCR using gene-specific primers. The PCR products were resolved on a syber safe-stained 2% agarose gel. No PCR products were detected after 40 cycles of amplification of cDNA from homozygous *atprx53* mutants, whereas specific amplifications were detected after amplification of cDNA from wild-type plants (L*er*). Arabidopsis *Actin8* was used an internal positive control.

insertional mutant line (*atprx53*) from the Cold Spring Harbor Laboratory mutant collection.[44,45] Sequence analysis revealed that the Ds transposon was inserted into the third exon (**Fig. 2A**). The mRNA expression level of *AtPRX53* was quantified in wild-type plants (L*er*) and the homozygous mutant line using qPCR. No *AtPRX53* mRNA was detected after 40 cycles of amplification of cDNA from homozygous mutant plants (**Fig. 2B**). Morphological analyses of *atprx53* mutant revealed a long hypocotyl phenotype relative to wild-type plants (**Fig. 3A**). We also discovered at least one 3-carpel silique in 68% of the *atprx53* mutant plants assayed (**Fig. 3B–E**) while this phenotype was entirely absent from the wild type (L*er*). In order to scrutinize this phenotype, we overexpressed the *AtPRX53* coding sequence in the *atprx53* mutant. The 3-carpel silique phenotype was partially rescued in that only 14% of the transgenic T1 plants exhibited this alteration, thereby validating this silique
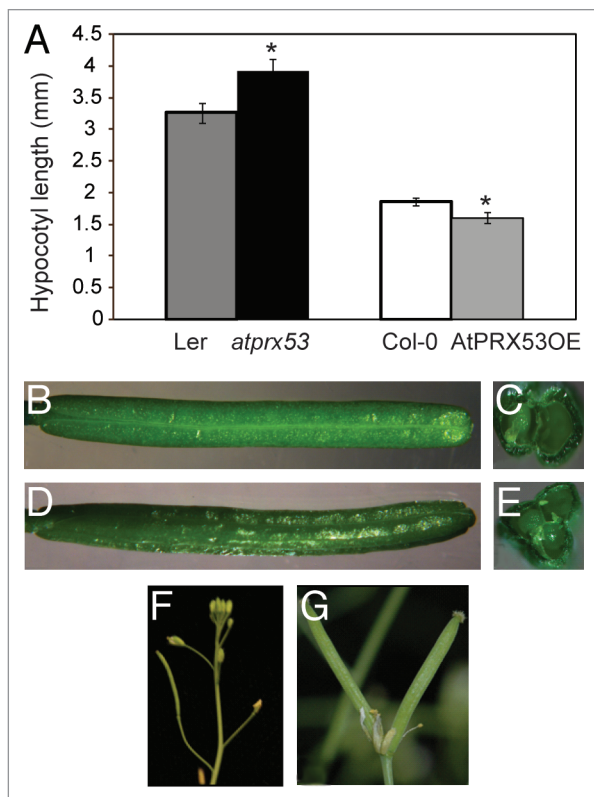
Figure 3. Phenotype of Arabidopsis lines with altered *AtPRX53* expression. (A) Hypocotyl length of the *atprx53* mutant and a representative transgenic Arabidopsis *AtPRX53* overexpression line (*AtPRX53*OE). Homozygous *atprx53* mutant and T$_3$ homozygous *AtPRX53*OE exhibited longer and shorter hypocotyls, respectively, than the corresponding wild type. Data are presented as means of 30 plants ± the standard error (SE). Asterisks indicate mean values significantly different from the wild type (p < 0.05). (B–G) Flower and silique phenotypes. Wild-type (L*er*) silique longitudinal view (B) and cross section (C) with two carpels. *atprx53* mutant silique longitudinal view (D) and cross section (E) with three carpels. Single wild-type (Col-0) silique (F) and *AtPRX53*OE double siliques (G).

phenotype as a consequence of the *atprx53* mutant allele despite its low penetrance.

In order to evaluate the influence of *AtPRX53* on nematode susceptibility, the *atprx53* mutant along with the wild type were subjected to cyst nematode susceptibility assays. Ten-day-old plants were inoculated with *H. schachtii* J2 nematodes and the number of J4 females was determined three weeks after inoculation and used to quantify plant susceptibility. As shown in **Figure 4A**, a trend of increased susceptibility of the *atprx53* mutant compared with the wild type was detected, although this increase was statistically non-significant. Because we found that reduced *AtPRX53* expression can affect both plant morphology and nematode susceptibility, it was particularly interesting to see whether elevated *AtPRX53* expression would produce opposite phenotypes. To investigate this, we generated transgenic lines overexpressing the *AtPRX53* coding sequence in the Col-0 background under the control of the CaMV 35S promoter. Three independent homozygous T$_3$ lines with confirmed *AtPRX53* mRNA abundance increases were phenotypically investigated.

In contrast to the *atprx53* mutant, *AtPRX53* overexpression lines exhibited significantly shorter hypocotyl lengths than the wild type (**Fig. 3A**). As was conducted for the *atprx53* mutant, we assayed *AtPRX53*-overexpressing T$_3$ lines along with wild-type plants for susceptibility to *H. schachtii* in four independent experiments. Compared with the wild type, *AtPRX53* overexpression plants exhibited reduced susceptibility to *H. schachtii* (**Fig. 4B**). We also discovered altered silique morphology. We reproducibly observed a double silique phenotype in *AtPRX53* overexpression lines albeit at a low frequency, i.e., ~5% of the tested plants showed at least one double silique (**Fig. 3F and G**).

AtPRX53 is not involved in lignification or ROS-mediated defense responses. As has been reported, AtPRX53 may function in lignifications.[21] We, therefore, tested the lignin deposition in the roots of the *AtPRX53* overexpression lines as compared with the wild type at 3, 8 and 14 dpi with *H. schachtii* using phloroglucinol staining, which produces a reddish color in lignified cells. No clear differences between the tested lines could be observed (**Fig. S1**). After nematode infection, lignin staining was visible around the nematode head in two genotypes but never in or around the syncytium, i.e., the location where we had observed strong *AtPRX53* promoter activity (**Fig. 1H and I**). We, therefore, conclude that AtPRX53 has no observable function in lignification during cyst nematode infection.

Peroxidases have been demonstrated to play a role in generating reactive oxygen species (ROS), which in turn function as signaling molecules in defense responses.[35,46] If AtPRX53 had a function in ROS generation then this activity should be reflected in changes of mRNA abundances of pathogenesis-related (*PR*) genes. In particular, *PR* genes should be upregulated in *AtPRX53* overexpression lines. To test this hypothesis, we quantified the expression level of seven *PR* genes (*PR1, PR2, PR3, PR4, PR6, PDF1.2* and *PAD4*) in the roots of *AtPRX53* overexpression lines and wild-type plants using qPCR. Data obtained from three independent experiments showed that the expression levels of *PR1, PR2* and *PR3* were similar to those in the wild type (**Fig. 5**), while *PR6* and *PDF1.2* were undetectable in roots. In contrast, *PR4* and *PAD4* showed significant downregulation in the roots of *AtPRX53* overexpression plants compared with the wild-type plants. Absence of upregulation of *PR* genes in the tested *AtPRX53* overexpression lines indicates that *AtPRX53* does not function in ROS-mediated activation of defense response signaling in roots during cyst nematode parasitism. In addition, quantification of ROS in the *AtPRX53* overexpression and wild-type plants using 3,3'-diaminobenzidine (DAB) showed no significant differences (data not shown) supporting the above conclusion.

Discussion

Secreted class III peroxidases represent a large plant protein family believed to be involved in a variety of physiological processes such as auxin catabolism, lignification, suberization, defense responses and cell wall cross-linking.[47] Functional characterization of individual isoforms is complicated because of genetic redundancies and low substrate specificities in vitro. In this study,
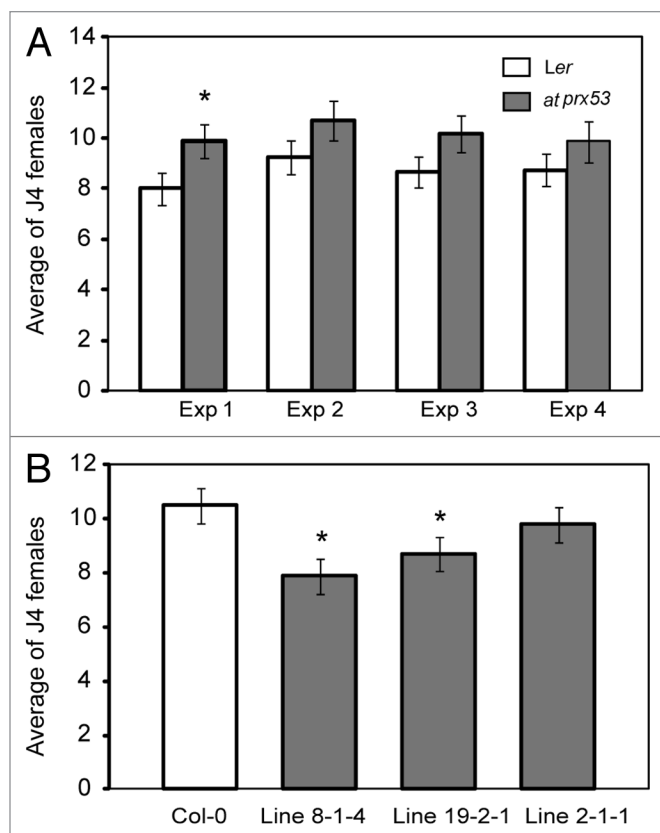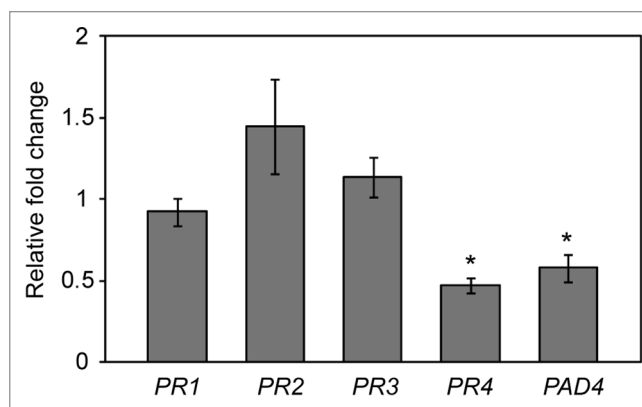
Figure 5. Pathogenesis-related (PR) gene expression in a representative Arabidopsis line overexpressing *AtPRX53* (*AtPRX53*OE). mRNA expression levels of PR genes were quantified by qPCR in root tissues of a representative *AtPRX53*OE line and wild-type plants 10 d after planting. Data are averages of three biologically independent experiments. *Actin8* was used as internal control to normalize mRNA expression levels. Mean values significantly different from the wild type were determined by unadjusted paired t-tests. Asterisks indicate mean fold-changes significantly different from wild-type roots ($p < 0.05$).

Figure 4. Nematode susceptibility assays of the *atprx53* mutant and three *AtPRX53*OE lines. (A) The *atprx53* mutant showed a consistent trend of increased susceptibility to *Heterodera schachtii* in four experiments (Exp) with Exp 1 showing statistically significant effects. (B) Two out of three *AtPRX53*OE lines showed significantly reduced susceptibility to *H. schachtii*. Arabidopsis plants were planted into 12-well plates containing modified Knop's medium, and ten-day-old plants were inoculated with ~200 surface-sterilized *H. schachtii* second-stage juveniles per plant. Three weeks after inoculation, the number of fourth-stage (J4) females per plant was determined. Mean values significantly different from the corresponding wild type were determined by modified t-test ($p < 0.05$).

we report on our work to determine the roles of *AtPRX53* in plant development and cyst nematode parasitism.

Using promoter-GUS fusion assays, we demonstrated that the *AtPRX53* promoter was active in the root vascular tissue, the sites of lateral root emergence as well as in the base of the flowers and maturing siliques. These spatial expression profiles are very similar to those obtained by Ostergaard et al.[21] suggesting a specific function in these organs. Because our qPCR studies revealed a significant increase of *AtPRX53* mRNA abundance early on during cyst nematode infection when penetration and migration through root tissues are associated with massive wounding of root tissues, we tested whether the expression of *AtPRX53* can be induced by wounding. In this experiment, we showed that the *AtPRX53* promoter in fact is wound-responsive. Wounding and pathogen responses share overlapping signaling pathways[48-50] in which JA is a key factor.[51] Therefore, we tested the *AtPRX53* expression in response to JA application and found that *AtPRX53*

expression was highly upregulated after JA treatment. This result is consistent with the existence of two JA-responsive cis-elements in *AtPRX53* promoter. In addition, *AtPRX53* promoter contains two abscisic acid response-like elements (ABRE motif, **Table 1**). While we did not test the function of these cis elements, several pieces of evidence indicate that the expression of some peroxidase genes is controlled by abscisic acid.[52,53] Whether nematodes-induce *AtPRX53* expression is abscisic acid-dependent needs further investigation.

However, when assaying GUS activity following cyst nematode infection, we documented higher GUS activity not only at the site of penetration or the migration path, but rather in the developing syncytium at 3 and 8 d post *H. schachtii* inoculation. Once the syncytium had assumed its maximum size (14 dpi), promoter activity largely ceased, demonstrating a role for *AtPRX53* only in the early stages of nematode infection when initiation and expansion of the syncytium are taking place. In other words, the role of *AtPRX53* during cyst nematode infection most likely is part of a classical plant wound response but also is associated directly with the growing syncytium.

Interestingly, the *atprx53* mutant showed a trend of non-significant increase of nematode susceptibility to cyst nematodes. In contrast, *AtPRX53* overexpression lines exhibited a reduced nematode susceptibility phenotype. These data provide a convincing reason to claim an important role of *AtPRX53* during plant-nematode interactions. Also, *atprx53* mutant and *AtPRX53* overexpression plants exhibited opposite morphological changes. While the *atprx53* mutant showed long hypocotyl and three-carpel silique phenotypes, the *AtPRX53* overexpression lines exhibited short hypocotyls as well as aberrant flower organ numbers in that two pistils originated from one flower. In agreement with Ostergaard et al.[21] we found that the *AtPRX53* promoter was highly active in the base tissues of flowers corroborating our

discovery of these morphological aberrations in the knockout and overexpression mutants. In other words, the three-carpel silique phenotype found in the *atprx53* mutant is most likely associated with the absence of *AtPRX53* activity, and the constitutive over-expression of *AtPRX53* resulted in morphological changes in the same tissue, asserting a likely function of *AtPRX53* in the formation of the Arabidopsis pistil.

AtPRX53, as an extracellular peroxidase, was first isolated from highly lignifying Arabidopsis cell suspension culture, suggesting a role of this gene in lignin biosynthesis.[21,54] However, we did not detect any clear lignin deposition differences between Arabidopsis lines with increased *AtPRX53* expression and the corresponding wild-type plants using phloroglucinol staining. Lignin deposition was only observed around the nematode head and to comparable degrees in all tested lines suggesting that *AtPRX53* does not play a major role in lignification during the expansion of the nematode feeding site.

Another known function of peroxidases is generating ROS in SA-, JA- or ET-mediated defense response pathways.[26] To test whether AtPRX53 functions in this manner, we quantified the expression of PR genes in *AtPRX53* overexpression plants using qPCR. None of the PR genes showed upregulation in the transgenic plants overexpressing *AtPRX53* relative to the wild type. In contrast, two PR genes, *PR4* and *PAD4*, exhibited significant downregulated indicating that *AtPRX53* likely is not involved in the generation of ROS and the activation of defense responses.

An additional possible role of *AtPRX53* is mediating cell growth through several different mechanisms.[55] First, peroxidases can activate cell elongation by generating ROS to cleave cell wall polymers, which loosens the cell wall, resulting in increased cell size.[56-58] As a second possibility, peroxidases can induce cell growth also through IAA signaling pathways.[46] i.e., Cosio et al.[24] found that transgenic Arabidopsis constitutively expressing a zucchini peroxidase, which showed an auxin oxidase activity in vitro, exhibited longer hypocotyl lengths than wild-type plants. In both cases, increased peroxidase activity led to increased cell size. However, our data showed the exact opposite phenotypes of short hypocotyls in the *AtPRX53* overexpression line and long hypocotyls in the mutant line, which argues against a role of *AtPRX53* in mediating cell elongation through cell wall loosening or auxin catabolism.

A shortened or lengthened hypocotyl is a clear indicator of reduced or activated cell elongation, respectively, as no further cell divisions are taking place in this plant tissue.[59] Our observation of reduced hypocotyl length in the *AtPRX53* overexpression lines and increased length in the *atprx53* mutant, therefore, suggested a strong negative effect of AtPRX53 on cell elongation. In fact, plant peroxidases have been reported to inhibit cell elongation by catalyzing cross linking of phenolic groups and proteins such as extensins[20,60] or compounds like ferulic acid, monolignol and aliphatic components.[19,61-63] The short and long hypocotyl phenotypes found in *AtPRX53* overexpression and *atprx53* mutant lines, respectively, provide strong support for the hypothesis that AtPRX53 could catalyze the cross linking of cell wall compounds to modulate, or potentially counteract, cell elongation. Such a role also makes sense with regard to the expression of *AtPRX53* in the

developing syncytium. After a competent cell is selected by the nematode, substantial cell wall changes and cell expansions occur as can be seen by the conspicuous swelling of Arabidopsis roots in the area of a syncytium. Cell wall cross linking during this phase appears to be a crucial component of controlled expansion of this novel plant organ. Once the syncytium is fully developed, the cell wall reorganization and extension discontinue and the expression of *AtPRX53* is inhibited, which is what we observed in our studies where the *AtPRX53* promoter was inactivated in the mature syncytium at 14 dpi. Consistent with this hypothesis, *AtPRX53* is not expressed in the zone of root elongation but becomes active only in adjacent older root tissues, i.e., when cells cease growth and their cell walls need to harden.

Such a scenario could also explain the reduced susceptibility of *AtPRX53* overexpression lines, which most likely is due to a reinforcement of cell walls, which could impede *H. schachtii* infection. The weak effect of *AtPRX53* overexpression on nematode susceptibility could be due to the fact that early reinforcement of cell walls was not strong enough to inhibit *H. schachtii* invasion. The fact that the Arabidopsis genome contains a high number of genes coding for peroxidases with likely redundant functions could explain the only slight effect of the *atprx53* mutant on nematode susceptibility. In this context, *AtPrx54* which shares 73% amino acid identity with *AtPRX53* in addition to several cis-regulatory elements[64] showed a considerable upregulation (~5 fold) at 3 dpi with *H. schachtii* (data not shown). This common transcriptional regulation in response to *H. schachtii* infection reinforces a potential role of these peroxidases in cell wall cross linking.

Materials and Methods

Plant materials and growth conditions. Arabidopsis [ecotype Columbia-0 (Col-0) and Landsberg *erecta* (L*er*)] were used in this study. Seeds were surface-sterilized in 50% commercial bleach with 0.1% Tween20 for 5 min followed by five washes in sterile water. Plants were grown on Murashige and Skoog (MS) medium (PlantMedia, Catalog: 30630067-1) containing 2% sucrose solidified with 0.8% Phyto Agar (Research Products International Corp., Catalog: A20300-1000.0) or in Metro-Mix 200 soil mixture (Sun Gro Horticulture) in a growth chamber (16 h light/8 h dark) at 23°C.

Identification of *atprx53* mutant. One Ds transposon insertional mutant (ET11708, *atprx53*) in the L*er* background was obtained from the Cold Spring Harbor Laboratory mutant collection.[44,45] Sequence analysis revealed that the Ds transposon element is inserted in exon 3,550 bp downstream of the translation start codon. The homozygosity of this mutant was verified using the primer pairs Forward/Ds3-4, Reverse/Ds5-4 and Foward/Reverse (**Table S1**) and the mRNA expression level was quantified by quantitative real-time RT-PCR (qPCR) using gene-specific primers for *AtPRX53* (**Table S1**).

Plasmid construction and generation of transgenic Arabidopsis lines. For the *AtPRX53* promoter:GUS (p*AtPRX53*:GUS) construct, a 986 bp fragment upstream of the translation start codon of the *AtPRX53* gene was amplified from

genomic DNA using primer pairs containing SalI and *BamH*I restriction sites in the forward and reverse primers, respectively (**Table S1**). PCR products were digested, gel purified and cloned into *Sal*I/*BamH*I sites of the binary vector pBI101. For the overexpression construct, the coding sequence of *AtPRX53* was amplified from Arabidopsis cDNA using gene-specific primers designed to create the *BamH*I and *Sac*I restriction sites in *AtPRX53* forward and reverse primers, respectively (**Table S1**). The amplified *AtPRX53* fragment was then cloned into the respective sites in the binary vector pBI121. All constructs were confirmed by sequencing and introduced into Arabidopsis by *Agrobacterium tumefaciens*-mediated transformation following the floral dip method.[65]

Nematode susceptibility assay. Arabidopsis seeds of transgenic homozygous T$_3$ lines, *atprx53* mutant and wild-type controls (Col-0 or L*er*) were surface sterilized and planted in a random block design in 12-well Falcon culture plates (BD Biosciences, Catalog: 353043) containing modified Knop's medium[66] solidified with 0.8% Daishin agar (Brunschwig Chemie, Catalog: A20350-1000.0). Plants were grown at 26°C under 16 h light/8 h dark conditions. Ten-day-old seedlings were inoculated with ~200 surface-sterilized J2 *Heterodera schachtii* as previously described by Baum et al.[67] Inoculated plants were maintained under the conditions described above. Three weeks post inoculation, the number of *H. schachtii* J4 females was counted using a dissecting microscope. Each plant line was replicated at least 15 times, and four independent experiments were performed. Average numbers of J4 females were calculated, and statistically significant differences between plant lines and the corresponding wild-type control were determined in a modified t-test using the statistical software package SAS.

Histochemical detection of GUS activity. The histochemical detection of GUS activity was performed with the substrate 5-bromo-4-chloro-3-indolylglucuronide (X-Gluc, Research Products International Corp., Catalog: B72200-1.0) according to Jefferson et al. At different time points post inoculation with *H. schachtii*, both infected and non-infected plants were stained with GUS solution at 37°C overnight. After GUS staining, plants were incubated in 70% ethanol to remove chlorophyll from the green tissues. Stained tissues were observed and photographed with a Zeiss Axiovert 100 microscope.

Wounding treatment. Wounding treatment was performed by repeatedly piercing whole Arabidopsis roots with a needle. Three days after wounding, whole roots were stained with GUS solution at 37°C overnight.

Quantitative real-time RT-PCR (qPCR). Total RNA was extracted from approximately 100 mg Arabidopsis roots using the RNAqueous kit (Ambion, Catalog: AM1912) following the manufacturer's instructions. Genomic DNA contamination was completely removed from the samples by DNase I (Invitrogen, Catalog: 18068-015) treatment. Gene-specific primers to

Arabidopsis *AtPRX53, PR1, PR2, PR3, PR4, PR6, PDF1.2, PAD4* and *Actin8* were designed and used in qPCR (**Table S1**). Gene expression levels were quantified in three independent biological samples, each consisting of four technical replicates. PCR reactions were run in an ICycler (Bio-Rad). PCR program and quantification of the relative changes in gene expression were conducted as previously described in reference 69.

Hypocotyl length measurement. For hypocotyl length measurement, Arabidopsis seeds were planted in Petri dishes (150 x 15 mm) containing modified Knop's medium. Plates were incubated vertically in a growth chamber at 26°C under 16 h light/8 h dark condition. Seven days after planting, the hypocotyl length of at least 30 plants per line was measured in three independent experiments. Statistically significant differences between transgenic line and the corresponding wild-type control were determined by unadjusted unpaired t-test (p < 0.05).

Phloroglucinol histochemical staining of Arabidopsis roots. Arabidopsis roots, collected at 3, 8 and 14 d post inoculation, were fixed overnight in FAA solution (50% ethonal:formaldehyde:acetic acid = 18:1:1) at 4°C. After removing fixation solution, 1% phloroglucinol solution was added to the roots for 5 min. Stained tissues were observed and photographed with a Zeiss Axiovert 100 microscope within 15 min of phloroglucinol staining.[70]

Hydrogen peroxide staining of Arabidopsis roots. *AtPRX53* overexpression and wild-type roots were treated with 1 mg/l 3,3'-Diaminobenzidine (DAB) (Acros Organics, Catalog: AC11209-0050) in 50 mM TRIS-acetate buffer, pH 5.0, at 25°C for 24 h in the dark.[71] Stained roots were observed under a Zeiss Axiovert 100 microscope.

Accession Numbers

AtPRX53: At5g06720, *PR1:* At2g14610, *PR2:* At3g57260, *PR3:* At3g12500, *PR4:* At3g04720, *PR6:* At2g38900, *PDF1.2:* At5g44420, *PAD4:* At3g52430 and *Actin8:* At1g49240.

References

1. Wrather JA, Anderson TR, Arsyad DM, Tan Y, Ploper LD, Porta-Puglia A, et al. Soybean disease loss estimates for the top ten soybean-producing countries in 1998. Can J Plant Pathol 2001; 23:115-21; DOI:10.1080/07060660109506918.

2. Davis EL, Hussey R, Baum T, Bakker J, Schots A, Rosso M, et al. Nematode parasitism genes. Annu Rev Phytopathol 2000; 38:365-96; PMID:11701847; DOI:10.1146/annurev.phyto.38.1.365.

3. Baum T, Hussey R, Davis E. Root-knot and cyst nematode parasitism genes: the molecular basis of plant parasitism. Genet Eng (NY) 2007; 28:17-43; PMID:17153931; DOI:10.1007/978-0-387-34504-8_2.

4. Hewezi T, Howe P, Maier T, Hussey R, Mitchum M, Davis E, et al. Cellulose binding protein from the parasitic nematode heterodera schachtii interacts with Arabidopsis pectin methylesterase: Cooperative cell wall modification during parasitism. Plant Cell 2008; 20:3080-93; PMID:19001564; DOI:10.1105/tpc.108.063065.

5. Hewezi T, Howe PJ, Maier TR, Hussey RS, Mitchum MG, Davis EL, et al. Arabidopsis Spermidine Synthase Is Targeted by an Effector Protein of the Cyst Nematode *Heterodera schachtii*. Plant Physiol 2010; 152:968-84; PMID:19965964; DOI:10.1104/pp.109.150557.

6. Patel N, Hamamouch N, Li C, Hewezi T, Hussey RS, Baum TJ, et al. A nematode effector protein similar to annexins in host plants. J Exp Bot 2010; 61:235-48; PMID:19887499; DOI:10.1093/jxb/erp293.

7. Gheysen G, Mitchum MG. Molecular insights in the susceptible plant response to nematode infection. Plant Cell Monographs 2009; 45-81.

8. Puthoff DP, Nettleton D, Rodermel S, Baum T. Arabidopsis gene expression changes during cyst nematode parasitism revealed by statistical analyses of microarray expression profiles. Plant J 2003; 33:911-21; PMID:12609032; DOI:10.1046/j.1365-313X.2003.01677.x.

9. Klink VP, Alkharouf N, MacDonald M, Matthews B. Laser capture microdissection (LCM) and expression analyses of *Glycine max* (soybean) syncytium containing root regions formed by the plant pathogen Heterodera glycines (soybean cyst nematode). Plant Mol Biol 2005; 59:965-79; PMID:16307369; DOI:10.1007/s11103-005-2416-7.

10. Klink VP, Overall C, Alkharouf N, MacDonald M, Matthews B. Laser capture microdissection (LCM) and comparative microarray expression analysis of syncytial cells isolated from incompatible and compatible soybean (Glycine max) roots infected by the soybean cyst nematode (Heterodera glycines). Planta 2007; 226:1389-409; PMID:17668236; DOI:10.1007/s00425-007-0578-z.

11. Ithal N, Recknor J, Nettleton D, Maier T, Baum T, Mitchum M. Developmental transcript profiling of cyst nematode feeding cells in soybean roots. Mol Plant Microbe Interact 2007; 20:510-25; PMID:17506329; DOI:10.1094/MPMI-20-5-0510.

12. Szakasits D, Heinen P, Wieczorek K, Hofmann J, Wagner F, Kreil D, et al. The transcriptome of syncytia induced by the cyst nematode *Heterodera schachtii* in Arabidopsis roots. Plant J 2009; 57:771-84; PMID:18980640; DOI:10.1111/j.1365-313X.2008.03727.x.

13. Welinder KG. Superfamily of plant, fungal and bacterial peroxidases. Curr Opin Struct Biol 1992; 2:388-93; DOI:10.1016/0959-440X(92)90230-5.

14. Shigeoka S, Ishikawa T, Tamoi M, Miyagawa Y, Takeda T, Yabuta Y, et al. Regulation and function of ascorbate peroxidase isoenzymes. J Exp Bot 2002; 53:1305-19; PMID:11997377; DOI:10.1093/jexbot/53.372.1305.

15. Martínez AT, Speranza M, Ruiz-Duenas FJ, Ferreira P, Camarero S, Guillen F, et al. Biodegradation of lignocellulosics: microbial chemical and enzymatic aspects of the fungal attack of lignin. Int Microbiol 2005; 8:195-204; PMID:16200498.

16. Hiraga S, Sasaki K, Ito H, Ohashi Y, Matsui H. A large family of class III plant peroxidases. Plant Cell Physiol 2001; 42:462-8; PMID:11382811; DOI:10.1093/pcp/pce061.

17. Tognolli M, Penel C, Greppin H, Simon P. Analysis and expression of the class III peroxidase large gene family in *Arabidopsis thaliana*. Gene 2002; 288:129-38; PMID:12034502; DOI:10.1016/S0378-1119(02)00465-1.

18. Duroux L, Welinder KG. The peroxidase gene family in plants: A phylogenetic overview. J Mol Evol 2003; 57:397-407; PMID:14708573; DOI:10.1007/s00239-003-2489-3.

19. Fry SC. Cross-linking of matrix polymers in the growing cell-walls of angiosperms. Annu Rev Plant Physiol Plant Mol Biol 1986; 37:165-86; DOI:10.1146/annurev.arplant.37.1.165.

20. Brownleader MD, Ahmed N, Trevan M, Chaplin M, Dey P. Purification and Partial Characterization of Tomato Extensin Peroxidase. Plant Physiol 1995; 109:1115-23; PMID:12228657.

21. Ostergaard L, Teilum K, Mirza O, Mattsson O, Petersen M, Welinder KG, et al. Arabidopsis ATP A2 peroxidase. Expression and high-resolution structure of a plant peroxidase with implications for lignification. Plant Mol Biol 2000; 44:231-43; PMID:11117266; DOI:10.1023/A:1006442618860.

22. Marjamaa K, Kukkola EM, Fagerstedt KV. The role of xylem class III peroxidases in lignification. J Exp Bot 2009; 60:367-76; PMID:19264758; DOI:10.1093/jxb/ern278.

23. Bernards MA, Fleming WD, Llewellyn DB, Priefer R, Yang XL, Sabatino A, et al. Biochemical characterization of the suberization-associated anionic peroxidase of potato. Plant Physiol 1999; 121:135-46; PMID:10482668; DOI:10.1104/pp.121.1.135.

24. Cosio C, Vuillemin L, De Meyer M, Kevers C, Penel C, Dunand C. An anionic class III peroxidase from zucchini may regulate hypocotyl elongation through its auxin oxidase activity. Planta 2009; 229:823-36; PMID:19116728; DOI:10.1007/s00425-008-0876-0.

25. Delannoy E, Jalloul A, Assigbetse K, Marmey P, Giger JP, Lherminier J, et al. Activity of class III peroxidases in the defense of cotton to bacterial blight. Mol Plant Microbe Interact 2003; 16:1030-8; PMID:14601671; DOI:10.1094/MPMI.2003.16.11.1030.

26. Almagro L, Ros LVG, Belchi-Navarro S, Bru R, Barcelo AR, Pedreno MA. Class III peroxidases in plant defence reactions. J Exp Bot 2009; 60:377-90; PMID:19073963; DOI:10.1093/jxb/ern277.

27. Lehtonen MT, Akita M, Kalkkinen N, Ahola-Iivarinen E, Ronnholm G, Somervuo P, et al. Quickly-released peroxidase of moss in defense against fungal invaders. New Phytol 2009; 183:432-43; PMID:19453432; DOI:10.1111/j.1469-8137.2009.02864.x.

28. Chassot C, Nawrath C, Metraux JP. Cuticular defects lead to full immunity to a major plant pathogen. Plant J 2007; 49:972-80; PMID:17257167; DOI:10.1111/j.1365-313X.2006.03017.x.

29. Diaz-Vivancos P, Rubio M, Mesonero V, Periago PM, Barcelo AR, Martinez-Gomez P, et al. The apoplastic antioxidant system in Prunus: response to long-term plum pox virus infection. J Exp Bot 2006; 57:3813-24; PMID:17043083; DOI:10.1093/jxb/erl138.

30. Little D, Gouhier-Darimont C, Bruessow F, Reymond P. Oviposition by pierid butterflies triggers defense responses in Arabidopsis. Plant Physiol 2007; 143:784-800; PMID:17142483; DOI:10.1104/pp.106.090837.

31. Simonetti E, Veronico P, Melillo MT, Delibes A, Andres MF, Lopez-Brana I. Analysis of class III peroxidase genes expressed in roots of resistant and susceptible wheat lines infected by *Heterodera avenae*. Mol Plant Microbe Interact 2009; 22:1081-92; PMID:19656043; DOI:10.1094/MPMI-22-9-1081.

32. Showalter AM. Structure and function of plant-cell wall proteins. Plant Cell 1993; 5:9-23; PMID:8439747; DOI: 10.1105/tpc.5.1.9.

33. Jackson PA, Galinha C, Pereira C, Fortunato A, Soares N, Amâncio S, et al. Rapid deposition of extensin during the elicitation of grapevine callus cultures is specifically catalyzed by a 40-kilodalton peroxidase. Plant Physiol 2001; 127:1065-76; PMID:11706187; DOI:10.1104/pp.010192.

34. Torres MA, Jones JDG, Dangl JL. Reactive oxygen species signaling in response to pathogens. Plant Physiol 2006; 141:373-8; PMID:16760490; DOI:10.1104/pp.106.079467.

35. Bindschedler LV, Dewdney J, Blee KA, Stone JM, Asai T, Plotnikov J, et al. Peroxidase-dependent apoplastic oxidative burst in Arabidopsis required for pathogen resistance. Plant J 2006; 47:851-63; PMID:16889645; DOI:10.1111/j.1365-313X.2006.02837.x.

36. Bolwell GP, Daudi A. Reactive oxygen species in plant-pathogen interactions. Reactive oxygen species in Plant Signaling 2009; 113-33.

37. Passardi F, Tognolli M, De Meyer M, Penel C, Dunand C. Two cell wall associated peroxidases from Arabidopsis influence root elongation. Planta 2006; 223:965-74; PMID:16284776; DOI:10.1007/s00425-005-0153-4.

38. Higo K, Ugawa Y, Iwamoto M, Korenaga T. Plant cis-acting regulatory DNA elements (PLACE) database: 1999. Nucleic Acids Res 1999; 27:297-300; PMID:9847208; DOI:10.1093/nar/27.1.297.

39. Boter M, Ruiz-Rivero O, Abdeen A, Prat S. Conserved MYC transcription factors play a key role in jasmonate signaling both in tomato and Arabidopsis. Genes Dev 2004; 18:1577-91; PMID:15231736; DOI:10.1101/gad.297704.

40. Montgomery J, Goldman S, Deikman J, Margossian L, Fischer RL. Identification of an ethylene-responsive region in the promoter of a fruit ripening gene. Proc Natl Acad Sci USA 1993; 90:5939-43; PMID:8327464; DOI:10.1073/pnas.90.13.5939.

41. Itzhaki H, Maxson JM, Woodson WR. An ethylene-responsive enhancer element is involved in the senescence-related expression of the carnation glutathione-s-transferase (GSTI) gene. Proc Natl Acad Sci USA 1994; 91:8925-9; PMID:8090746; DOI:10.1073/pnas.91.19.8925.

42. Nakashima K, Fujita Y, Katsura K, Maruyama K, Narusaka Y, Seki M, et al. Transcriptional regulation of ABI3-and ABA-responsive genes including RD29B and RD29A in seeds, germinating embryos and seedlings of Arabidopsis. Plant Mol Biol 2006; 60:51-68; PMID:16463099; DOI:10.1007/s11103-005-2418-5.

43. Escobar C, De Meutter J, Aristizabal FA, Sanz-Alferez S, del Campo FF, Barthels N, et al. Isolation of the LEMM19 gene and promoter analysis during a compatible plant-nematode interaction. Mol Plant Microbe Interact 1999; 12:440-9; PMID:10226377; DOI:10.1094/MPMI.1999.12.5.440.

44. Martienssen RA. Functional genomics: Probing plant gene function and expression with transposons. Proc Natl Acad Sci USA 1998; 95:2021-6; PMID:9482828; DOI:10.1073/pnas.95.5.2021.

45. Sundaresan V, Springer P, Volpe T, Haward S, Jones JDG, Dean C, et al. Patterns of gene-action in plant development revealed by enhancer trap and gene trap transposable elements. Genes Dev 1995; 9:1797-810; PMID:7622040; DOI:10.1101/gad.9.14.1797.

46. Kawano T. Roles of the reactive oxygen species-generating peroxidase reactions in plant defense and growth induction. Plant Cell Rep 2003; 21:829-37; PMID:12789499; DOI: 10.1007/s00299-003-0591-z.

47. Cosio C, Dunand C. Specific functions of individual class III peroxidase genes. J Exp Bot 2009; 60:391-408; PMID:19088338; DOI:10.1093/jxb/ern318.

48. Maleck K, Dietrich R. Defense on multiple fronts: how do plants cope with diverse enemies? Trends Plant Sci 1999; 4:215-9; PMID:10366877; DOI:10.1016/S1360-1385(99)01415-6.

49. Reymond P, Weber H, Damond M, Farmer EE. Differential gene expression in response to mechanical wounding and insect feeding in Arabidopsis. Plant Cell 2000; 12:707-20; PMID:10810145; DOI: 10.1105/tpc.12.5.707.

50. Cheong YH, Chang H, Gupta R, Wang X, Zhu T, Luan S. Transcriptional profiling reveals novel interactions between wounding, pathogen, abiotic stress and hormonal responses in Arabidopsis. Plant Physiol 2002; 129:661-77; PMID:12068110; DOI:10.1104/pp.002857.

51. Dong X. JA, ethylene and disease resistance in plants. Curr Opin Plant Biol 1998; 1:316-23; PMID:10066607; DOI:10.1016/1369-5266(88)80053-0.

52. Schopfer P, Plachy C, Frahry G. Release of reactive oxygen intermediates (superoxide radicals, hydrogen peroxide and hydroxyl radicals) and peroxidase in germinating radish seeds controlled by light, gibberellin and abscisic acid. Plant Physiol 2001; 125:1591-602; PMID:11299341; DOI:10.1104/pp.125.4.1591.

53. Lin CC, Kao CH. Abscisic acid induced changes in cell wall peroxidase activity and hydrogen peroxide level in roots of rice seedlings. Plant Sci 2001; 160:323-9; PMID:11164604; DOI:10.1016/S0168-9452(00)00396-4.

54. Ostergaard L, Abelskov AK, Mattsson O, Welinder KG. Structure and organ specificity of an anionic peroxidase from Arabidopsis thaliana cell suspension culture. FEBS Lett 1996; 398:243-7; PMID:8977116; DOI:10.1016/S0014-5793(96)01244-6.

55. Passardi F, Penel C, Dunand C. Performing the paradoxical: how plant peroxidases modify the cell wall. Trends Plant Sci 2004; 9:534-40; PMID:15501178; DOI:10.1016/j.tplants.2004.09.002.

56. Cordoba-Pedregosa M, Gonzalez-Reyes J, Canadillas M, Navas P, Cordoba F. Role of Apoplastic and Cell-Wall Peroxidases on the Stimulation of Root Elongation by Ascorbate. Plant Physiol 1996; 112:1119-25; PMID:12226436; DOI: 10.1104/pp.112.3.1119.

57. Fry SC. Oxidative scission of plant cell wall polysaccharides by ascorbate-induced hydroxyl radicals. Biochem J 1998; 332:507-15; PMID:9601081.

58. Schweikert C, Liszkay A, Schopfer P. Scission of polysaccharides by peroxidase-generated hydroxyl radicals. Phytochemistry 2000; 53:565-70; PMID:10724181; DOI:10.1016/S0031-9422(99)00586-5.

59. Gendreau E, Traas J, Desnos T, Grandjean O, Caboche M, Höfte H. Cellular basis of hypocotyl growth in Arabidopsis thaliana. Plant Physiol 1997; 114:295-305; PMID:9159952; DOI:10.1104/pp.114.1.295.

60. Ahmed N, Chaplin M, Trevan M, Dey P, Brownleader M. Purification and partial characterization of 'extensin peroxidase'. Biochem Soc Trans 1995; 23:154; PMID:7672185.

61. Macadam JW, Nelson CJ, Sharp RE. Peroxidase-activity in the leaf elongation zone of tall fescue. (1) spatial-distribution of ionically bound peroxidase-activity in genotypes differing in length of the elongation zone. Plant Physiol 1992; 99:872-8; PMID:16669014; DOI:10.1104/pp.99.3.872.

62. Warneck HM, Haug T, Seitz U. Activation of cell wall-associated peroxidase isoenzymes in pea epicotyls by a xyloglucan-derived nonasaccharide. J Exp Bot 1996; 47:1897-904; DOI:10.1093/jxb/47.12.1897.

63. Wallace G, Fry SC. Action of diverse peroxidases and laccases on six cell wall-related phenolic compounds. Phytochemistry 1999; 52:769-73; DOI:10.1016/S0031-9422(99)00342-8.

64. Cosio C, Dunand C. Specific functions of individual class III peroxidase genes. J Exp Bot 2009; 60:391-408; PMID:19088338; DOI:10.1093/jxb/ern318.

65. Clough SJ, Bent A. Floral dip: a simplified method for Agrobacterium-mediated transformation of Arabidopsis thaliana. Plant J 1998; 16:735-43; PMID:10069079; DOI:10.1046/j.1365-313x.1998.00343.x.

66. Sijmons P, Grundler F, Mende N, Burrows PR, Wyss U. Arabidopsis thaliana as a new model host for plant-parasitic nematodes. Plant J 1991; 1:10; DOI:10.1111/j.1365-313X.1991.00245.x.

67. Baum TJ, Wubben MJE, Hardy KA, Su H, Rodermel SR. A screen for Arabidopsis thaliana mutants with altered susceptibility to Heterodera schachtii. J Nematol 2000; 32:166-73; PMID:19270962.

68. Jefferson RA, Kavanagh TA, Bevan MW. GUS fusions—beta-glucuronidase as a sensitive and versatile gene fusion marker in higher-plants. EMBO J 1987; 6:3901-7; PMID:3327686.

69. Livak KJ, Schmittgen TD. Analysis of relative gene expression data using real-time quantitative PCR and the 2(T)(-Delta Delta C) method. Methods 2001; 25:402-8; PMID:11846609; DOI:10.1006/meth.2001.1262.

70. Newman LJ, Perazza DE, Juda L, Campbell MM. Involvement of the R2R3-MYB, AtMYB61, in the ectopic lignification and dark-photomorphogenic components of the det3 mutant phenotype. Plant J 2004; 37:239-50; PMID:14690508; DOI:10.1046/j.1365-313X.2003.01953.x.

71. Einset J, Nielsen E, Connolly E, Bones A, Sparstad T, Winge P, et al. Membrane-trafficking RabA4c involved in the effect of glycine betaine on recovery from chilling stress in Arabidopsis. Physiol Plant 2007; 130:511-8; DOI:10.1111/j.1399-3054.2007.00920.x.